The following supplement accompanies the article

Multi-disciplinary fingerprints reveal the harvest location of cod *Gadus morhua* in the northeast Atlantic

Ruth M. Higgins[1,11,*], Bret S. Danilowicz[1,2], Juan A. Balbuena[3], Anna K. Daníelsdóttir[4,10], Audrey J. Geffen[5], Wim G. Meijer[6], Johan Modin[7], Francisco E. Montero[3,9], Christophe Pampoulie[4], Diana Perdiguero-Alonso[3], Arnd Schreiber[8], Magnús Ö. Stefánsson[4], Bryan Wilson[1,6]

[1]School of Biological and Environmental Sciences, University College Dublin, Belfield, Dublin 4, Ireland
[2]College of Science and Technology, Georgia Southern University, Statesboro, Georgia 30458, USA
[3]Cavanilles Institute of Biodiversity and Evolutionary Biology, University of Valencia, PO Box 22085, 46071 Valencia, Spain
[4]Marine Research Institute, Skúlagata 4, 101 Reykjavik, Iceland
[5]Deptartment of Biology, University of Bergen, PO Box 7803, 5020 Bergen, Norway
[6]School of Biomolecular and Biomedical Sciences, University College Dublin, Belfield, Dublin 4, Ireland
[7]Coastal Research Institute, Swedish Board of Fisheries, 74071 Öregrund, Sweden
[8]University of Karlsruhe, Adenauerring 20, Geb. 50.40, 76131 Karlsruhe, Germany
[9]Department of Animal Biology, Plant Biology, and Ecology, Autonomous University of Barcelona, Campus Universitari, 08193 Bellaterra, Barcelona, Spain
[10]Matis, Skúlagata, 101 Reykjavík, Iceland
[11]Instituto do Mar, Universidade dos Açores, Horta, 9901-862, Portugal
*Email: ruth@uac.pt

Marine Ecology Progress Series 404: 197–206 (2010)

Supplement. Detailed methodology and approaches

1. COLLECTION OF COD

All fish were processed at the point of capture, either on scientific research vessels during groundfish surveys in the case of wild fish, or on location at the fish farms. Therefore, samples were processed immediately after collection. Each fish was assigned an individual identification code, which ensured that biological samples for each individual were distinctive. Mucus samples were collected from the external body surface and buccal cavity of the fish for analysis of bacterial assemblages; gill filaments were taken for microsatellite analysis; and various external body measurements were collected for morphometric synthesis. Total and standard lengths were also taken. Parasites were removed and preserved from the external and internal body surfaces, and the entire viscera including the gill arches of each fish were removed and stored for further identification of internal parasites. Both saggital otoliths were also collected from each fish. The left otolith was used to investigate otolith morphometry and for age determination, whereas the right otolith was used to determine the chemical composition both at the core and on the surface of the structure. Age and standard length information were later used to standardise elemental and parasite data where a significant age or size effect was detected.

1.1. Fish farm conditions

Farmed fish from Iceland were caught in Icelandic water as larvae and reared in tanks (150 l black silos). Food consisted of rotifers (Day 3 to 30), artemia (Day 25 to 60), dry food preparations. Algae and live food was provided 2× per day. The light regime included light and dark periods (darkness 3 d, continuous light, 500 lux at surface). Water temperature was maintained at 9 to 10°C. A chemical treatment Neobiotic (Neomycin, Streptocillin) was applied 1× per wk.

Scottish broodstock were farm reared in a variety of tanks (2 to 8 m in diameter). Parent fish were caught off Orkney, the west coast of Scotland and in the North Sea. Fish were fed on a diet of rotifers (Day 3 to 30) and DHA enriched artemia (Day 25 to 60). Dry feed was introduced from Day 50, and when weaning was complete the fish were moved to juvenile rearing tanks. Both home-cultured and commercial algae were used with the live feeds and in larvae tanks. After hatching, larvae were kept in continuous light (10 lux). Water

temperature was gradually increased from 6°C for incubation to 10°C after hatch. There was no routine use of antibiotics.

2. ANALYTICAL TECHNIQUES

2.1. Body morphometrics

A total of 23 measurements that together provide a truss network were taken from each fish by calliper recording (Strauss & Bookstein 1982). The truss consists of the following measures (see Fig. S1):

AB: Distance snout tip to front margin of orbit
BC: Orbit diameter
CD: Rear margin of the orbit to the front end of first dorsal fin
CE: Rear margin of the orbit to the rear end of operculum
CF: Rear margin of the orbit to the front end of pectoral fin
CG: Rear margin of the orbit to the front end of pelvic fin
ED: Rear end of the operculum to the front end of first dorsal fin
DF: Front end of first dorsal fin to front end of pectoral fin
FG: Front end of pectoral fin to front end of pelvic fin
DI: Front end of first dorsal fin to rear end of first dorsal fin
FH: Length of pectoral fin
GM: Front end of pelvic fin to front end of first anal fin
IM: Rear end of first dorsal fin to front end of first anal fin
IJ: Rear end of first dorsal fin to rear end of second dorsal fin
MN: Front end of first anal fin to rear end of first anal fin
JN: Rear end of second dorsal fin to rear end of first anal fin
JK: Rear end of second dorsal fin to rear end of third dorsal fin
NO: Rear end of first anal fin to rear end of second anal fin
KO: Rear end of third dorsal fin to rear end of 2nd anal fin
KL: Rear end of third dorsal fin to rear end of rump
OL: Rear end of second anal fin to rear end of rump
PP: Distance between the eyes (orbital margins)
QQ: Mouth width

Size-related allometry was investigated for all variables from the truss network. Body size in 12 of the 42 tested sex-specific collectives deviated from the normal distribution. A linear model confirmed that both age and geographical origin influenced body shape of cod significantly, the former being more important than the latter. Evidently, a heterogeneous array of age stages was collected even at the local scale of single collection sites. While some morphologists recommend the use of size-untransformed variables for morphometric evaluation, in order to prevent the introduction of biased precision into covariate parameters, a heterogeneously composed dataset like the present one necessitates correction for the ontogenetic growth if the geographical allocation of cod is aimed at. The following stratified procedure was therefore employed in further analysis:

1. Performing a principal component analysis (PCA), which was expected to separate size and shape para-

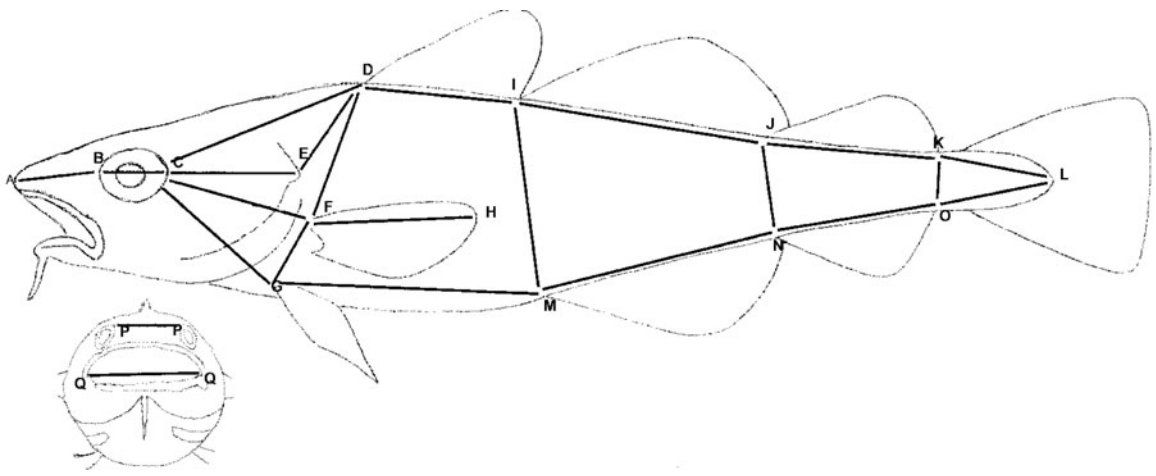

Fig. S1. Truss network of measurements made on each individual fish. The distribution of standard lengths in either sex (Kolmogorov-Smirnov tests, $p < 0.00001$), but not their variance (Levene test), departed significantly from the normal distribution. The standard length of females was significantly smaller than of males (Mann-Whitney *U*-test, $p = 0.02$). This sex dimorphism was seen in other measures as well and required the separate treatment of male and female cod in further evaluations

meters in different factors, with measurements that have not been standardized to a common body length.

2. Allometric size adjustment methods were applied for males and females separately, to treat for different growth patterns of the 22 measures considered, and of the 2 sexes. The possibility of different allometry in different geographical origins could not be considered because growth allometry, as such, had to be inferred from the overall dataset since *a priori* data were not available for cod. This theoretical limitation was not deemed to be a severe restriction, however, because external evidence (genetic data) showed that cod populations are genetically very cohesive across the entire study area. While body size itself might differ among the 8 geographical origins, this difference could provide a very useful and practically valuable marker for geographical assignment, and its elimination from the database by size-standardization would not be desirable.

3. Exploratory analysis of means and variances of untransformed data for single and for combined population samples suggests that a few of the measurements were prone to reading errors, or to misleading variance, and thus had to be removed from the analysis at this early stage. This affects body weight, and mouth width. Since standard length was applied only for size adjustment, and total length not at all, the further morphometric analysis rests on 22 measures from the truss panel (see Fig. S1).

Principal component extraction in factor analysis grouped the geographical test groups according to the spatial location of the collection sites, but only when considering 1 principal component out of 5 that explains 2.5% of the morphometric variance. Body size variance alone, chiefly due to growth, accounted for 95.5% of the morphological variation. Morphometric data that had been standardized by means of allometric growth functions for every size variable alone yielded less satisfactory assignment rates than did size-adjusted data that were in addition analyzed separately for every single year class. The dual control of ontogenetic shape transformation by (i) estimating the fishes' life age from otolith diagnosis and (ii) size-adjustment of raw data is proposed in order to assign individuals to geographical populations. If life ages are known, year classes permit geographical assignment even without size standards. Within the truss system of measurements taken in every cod specimen, most body size variables are inter-correlated, but orbital diameter and occiput length retain a certain independence of the remaining measurements.

The following adjustment formula was used to care for the size-related ontogenetic allometry of each of the 22 measures, considered separately in male and in female cod:

$$M_t = M_o\,(L_s/L_o)^b$$

In this formula M_t denotes the transformed measure; M_o the observed measure; L_s the mean standard length of either males of females across all population samples; and L_o the standard length of the individual under consideration.

The sex-specific regression coefficient b has been determined for each measure and for each sex separately. For doing so, log M_o was referred to log L_o.

2.2. Otolith morphometrics

The valid right-hand otoliths were cleaned with distilled water and thereafter stored and distributed in acid washed plastic trays.

Digitised images of valid otoliths were derived from an image analysis system developed by IMAGIC (Van Heel et al. 1996). The system consists of a standard stereomicroscope (Olympus SZX9) equipped with a digital camera (Leica D50) and connected to a computer. Image software was then used to produce images of 768 × 582 pixels. Calibration of area and *x*- and *y*-axis were done with a photographic film displaying a 1 mm area scale. All otolith images and calibration measurements were made at 6.3× magnification. The otoliths were placed under the microscope with the sulcus side upwards and oriented with the posterior part into the 4th quadrant. Transmitted light was used to obtain a dark silhouette of the otolith. Light intensity was monitored to yield a constant high contrast between dark and light. Images were taken (Fig. S2) and stored as data files together with text files that contained sample and image processing information.

Specific image software (IMAGIC version 5) was used to estimate the outer contour line by standard filtering and edge finding algorithms (Van Heel et al. 1996). Each otolith contour typically consisted of around 2000 Cartesian coordinates, which were interpolated to a standard of 4096 coordinates. These were subjected to Fourier transformation (discussed below) in order to yield the associated Fourier shape descriptors, commonly called harmonics. Otolith orientation was normalised by a 2-step Fourier transform and otolith size was normalised by division of each Fourier descriptor by the amplitude of the fundamental (2nd) Fourier descriptors. The derived descriptor constants were then used for the statistical analysis of otolith shapes. When illustrations were needed, the otolith shapes were reconstructed from the descriptor constants by inverse Fourier transforms (Fig. S2).

It should be noted that Fourier transforms can be applied along 2 different approaches. This can be illus-

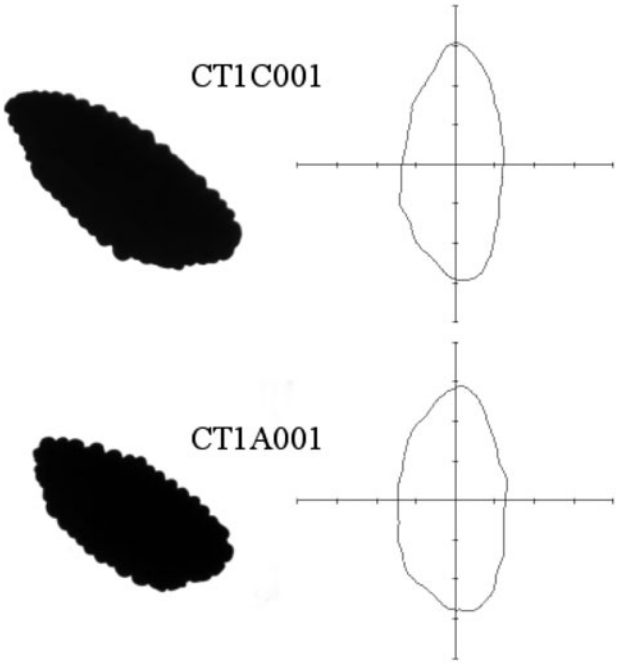

Fig. S2. Two otolith silhouettes (left) and the corresponding normalized otolith contours (right) that were recreated from 34 Fourier harmonics. The codes indicate fish ID

trated by the inverse Fourier transforms, i.e. the recreation of otolith contours from the calculated Fourier shape descriptors. One possibility is to describe the otolith shape as set of radii at equal angular intervals. This approach has been common in publications on otolith shapes (e.g. Campana & Casselman 1993), but it has 3 major drawbacks. One difficulty is to describe reentrant angles, a common feature in contours or profiles that form loops. The second issue is the need to initially define a centroid of a shape. The third problem is that statistical interference of shapes becomes complicated by the need for sophisticated analysis of circular data, i.e. the phase angle coefficients (Campana & Casselman 1993).

These problems are avoided if the Fourier transform and its inverse formulation are described mathematically as complex numbers (Smith et al. 2002, Galley et al. 2006, Ponton 2006). In this approach, which was adopted in the present study, the boundary of a shape is circumvented in constant intervals of a defined constant distance. The total distance of the perimeter is set to 2π and the intervals to 2^k (e.g. in this study: $k = 12$, i.e. $2^{12} = 4096$ intervals are used). Thus, increasing cumulative Fourier descriptor series can be used to describe a successively more complex contour, starting from a circle and in our case ending with a representation of the otolith contour.

The resulting Fourier coefficients were used for a statistical analysis of otolith shape. Note that by convention the index n of the Fourier descriptors range from negative to positive indexes. It has generally been observed that few (<20) Fourier descriptors are sufficient to describe otolith contours (Campana & Casselman 1993, Begg & Brown 2000, Cardinale et al. 2004). In the present study, coefficients for 33 descriptors were calculated, which yielded $2 \times 33 = 66$ coefficients per otolith shape. The first 2 Fourier descriptors were standardised to equal values and were consequently not used in the analysis.

The frequency distribution of each of the 66 coefficients within sample periods were tested for normality by the Kolmogorov-Smirnov one sample test (2-tailed test, $\alpha = 0.05$). There were only 4 coefficients that had non-normal frequency distributions. These coefficients were excluded from further statistical analysis.

2.3. Microsatellite DNA

DNA samples were extracted from gills or fin clips using a Chelex (small piece of tissue + 150 µl of 10% Chelex resin solution boiled 1 h) extraction protocol (Walsh et al. 1991). Samples were genotyped at 10 polymorphic microsatellite loci: Gmo2, Gmo132 (Brooker et al. 1994), Gmo8, Gmo19, Gmo34, Gmo35 (Miller et al. 2000), Tch5, Tch11, Tch14, and Tch22 (O'Reilly et al. 2000). Polymerase chain reactions (PCR) were performed in a 10 µl volume containing 2 µl of DNA product, 1 µl of 10µ Buffer (10 mM Tris-HCl, 50 mM KCl, 1.5 mM $MgCl_2$ and 0.1% Triton X-100), 1 µl of 2.5 mM DNTP, 0.2 to 0.4 units of DyNAzyme™ DNA polymerase (Finnzyme, 0.15 µl of 2 U ml^{-1}) and various concentrations of primers (0.4 to 1 µl of 10 nM working solution). PCR cycles were performed in a GeneAmp®2700 thermal block and preceded by an initial denaturation step of 4 min at 94°C followed by 32 cycles of: 40 s at 94°C, 40 s at annealing temperature (49 to 56°C), and 40 s at 72°C. A final elongation step of 4 min at 72°C was performed. PCR products were diluted with distilled water (1/3) screened in multiplexes on 25 cm 6% polyacrylamide gels and detected on an ABI-automatic sequencer (ABI 377, Applied Biosystems) using the software GeneScan version 3.1.2 (Applied Biosystems, 2000). Products were scored using the software GeneMapper version 3.0 (Applied Biosystems, 2002) several times to avoid scoring errors.

2.4. Parasites

The body cavity, liver surface and musculature (anisakid nematode larvae), viscera, gills, and gall bladder were examined. The multidisciplinary ap-

proach of the present study, and the other markers chosen, prohibited the detection of known cod parasite biomarkers such as the metacercaria of the bucephalid *Prosorhynchoides gracilescens* or the nostril copepod *Holomobolochus confusus* (Hemmingsen & MacKenzie 2001) since the fish heads were needed in the collection of other material and could not be studied for parasites in detail.

A total of 58 parasite species (or forms) occurred in the 1126 cod surveyed for parasites. Species with prevalence equal or lower than 1% were omitted since they were considered unpredictable, acting as a source of noise in the predictive analysis. In addition, species with prevalence equal or lower than 10% were carefully screened for their distribution across localities. Only those either occurring in a single locality or showing much higher abundance in a given locality than in the rest were retained for further analyses, since they might be useful to discriminate fish from that locality.

Two types of statistical analyses were performed to predict harvest location of cod: a supervised neural network based on a Bayesian backpropagation algorithm (hereafter BBP network) and a non-parametric version of linear discriminant analysis (LDA) consisting in applying a conventional LDA to rank-transformed data. This procedure seems appropriate to parasite data because it seems robust to violations of the assumptions of multinormality and homoscedasticity required in parametric LDA (Conover 1999). In all cases normality was tested using the Kolmogorov-Smirnov statistic. Although normality ($p \leq 0.05$) was achieved for some species' variables (WF: 7 out of 10 species, WW: 5 out of 10 species, FF: behaved binomially in many due to sparse data), this was not considered to be a major drawback since normality was not a pre-condition of BBP analysis and non-parametric LDA is more robust to such deviations.

The BBP networks were built with log-transformed parasite abundances [$\log_{10}(x + 1)$] using Neural Connection 2.0 (SPSS 1999). A number of different configurations were tried to determine the optimal models. Eventually, the BBP models chosen consisted in single hidden layer networks, whose number of nodes was determined automatically by the program; the input data were normalized prior to analysis, and the learning parameters were adapted during training following the automatic relevance detection mode. In each run, 2 BBP networks starting from different learning parameters were trained, being that yielding the best cost function eventually selected.

The LDAs with rank-transformed parasite abundances were run with SPSS 11.5 (SPSS), using the within-group co-variance matrix, and being the prior probability of cod belonging to a given group computed according to group size.

2.5. Microbiology

Bacterial communities colonising fish mucus were analysed by terminal restriction length polymorphism (TRFLP). TRFLP is an automated method in which fluorescently labelled 16S rRNA genes derived from bacterial populations from wild-caught and farm-reared cod mucus are digested with a frequently cutting restriction enzyme. The fragment lengths of the digested genes are subsequently analysed with a Beckman CEQ2000 automatic sequencer. Since the position of the restriction site within the 16S rRNA gene is unique for a particular species, the length of the fluorescent restriction fragments varied accordingly, which showed as a number of peaks in a chromatogram; an indicator of the diversity of the bacterial community. The height of the peak (fluorescence) is determined by the abundance of a species within the community. Therefore, together these data formed a molecular fingerprint of the bacterial community present in mucus produced by each fish. Identification of bacterial species was achieved by comparison of the sequence data to existing 16S rRNA databases. Mucus samples were taken from both the body surface and the buccal cavity of each fish.

Extraction of bacterial genomic DNA from cod mucus was performed using Qiagen Biorobot 3000 and Qiagen Blood DNA kit. Lysosyme (4 µl, 100 mg ml^{-1}) and 180 µl buffer ATL were added to mucus samples (suspended in 200 µl 10mM Tris-EDTA), shaken and incubated for 30 min at 37°C. Proteinase K (20 µl, 20 mg ml^{-1}) added to samples and incubated for 2 h at 56°C. Buffer AL (200 µl) added and samples incubated for 10 min at 70°C. Ethanol (200 µl, 98% v/v, stored at –20°C) added and samples placed at 4°C for 30 min. Samples applied to QIAamp filters and filtered using a vacuum manifold, washed with 500 µl Buffers AW1 and AW2, and eluted with 60 µl buffer AE. Genomic DNA was stored at –20°C.

PCR-amplified DNA applied to MinElute plates and filtered using a vacuum manifold at 800 bar for 10 min. Distilled water (30 µl) added to each well and plates shaken for 2 min at 200 rpm. Eluate removed from MinElute plates and transferred to clean 96 well PCR plates.

Cleaned PCR products diluted 20-fold in distilled water and Pico Green dye (diluted 200-fold in 1× TAE) added as per manufacturer's instructions and incubated for 3 min at 25°C before quantification. DNA was quantified using a Wallac Fluorescent Microplate Reader at 485 nm (excitation) and 535 nm (emission). DNA concentration output data was then used by the Qiagen Biorobot 3000 to normalise concentrations of DNA prior to digestion.

Msp1 (10 units) and 10× buffer were prepared in a mastermix, added to normalised PCR-amplified DNA

using the Qiagen Biorobot 3000, and incubated at 37°C for 2 h.

Samples were filtered using Qiagen DyeEx 96 kits and eluates dried in a vacuum drier. Dried DNA was resuspended in deionised formamide (5 µl). Size-standard-600 DNA ladder (0.2 µl) and sample DNA (0.4 µl) were added to deionised formamide (40 µl), and fragment analysis performed on a Beckman CEQ2000 Sequencer. Fragment data was analysed using a quartic equation with Beckman CEQ2000 Fragment Analysis software. T-RFLP profiles (fragment size and peak area) were exported to spreadsheet (Microsoft Excel) form for statistical analysis.

Sample T-RFLP data was transformed into binary data (on the basis of a presence or absence of peak data), and any fragment found to appear rarely (i.e. once only) was removed from the data set prior to statistical analysis. The data set was then subjected to a Jaccard similarity analysis using Systat 8.0 (SPSS) and jack-knifed classification matrices calculated.

For use of the bacterial community data with DFA, the homogeneity of variance-covariance matrices was examined for each grouping (season and collection location) using scatterplots of the first 2 canonical discriminant functions. In each plot, there was an approximate equality in the overall size of the scatterplots, which is evidence of homogeneity of variance-covariance matrixes (Tabachnick & Fidell 1996). DFA is robust to violations of normality and sensitive mainly to the presence of outliers in the data set. Due to the transformation of the bacterial community data to presence/absence values for any given species, no outliers were present in the data matrix.

2.6. Otolith chemistry

Otoliths were extracted from the fish at the final stage of tissue sampling for multiple markers. Plastic forceps were used to extract the otoliths, and they were wiped clean and stored dry in plastic multi-cell trays. To reduce contamination during collection, all equipment was acid-washed, and the otoliths were handled using gloves. Later, otoliths were physically cleaned with a plastic brush, dipped in HNO_3, and rinsed in Milli-Q water. They were then stored in a dessicator to keep them clean.

The otoliths from all the samples were embedded in a clear epoxy resin (Araldite 212), which is suitable for histological work. The methods for embedding and sectioning large numbers of otoliths were employed, to allow the standardisation of the technique. Up to 40 cod otoliths were mounted in a single block of epoxy and sectioned with a computerised circular saw. The lubricating fluid was replaced with Milli-Q water to reduce the contamination of samples during sectioning. Subsequently, the strips of otoliths in resin were mounted onto glass slides; the number of otoliths on each slide was maximised to improve the efficiency of the LA-ICPMS analyses. Wherever possible, the combination of otoliths on the slides and the order of analysis were randomised to reduce any session or sequence effects in the results (Fig. S3). The preparation was then polished first with silicon carbide polishing film and then with diamond suspension to produce a clean, flat, and level sample surface for optimal focusing of the laser.

The elemental analysis of the cod otoliths was carried out using the high resolution ICP MS (Thermo

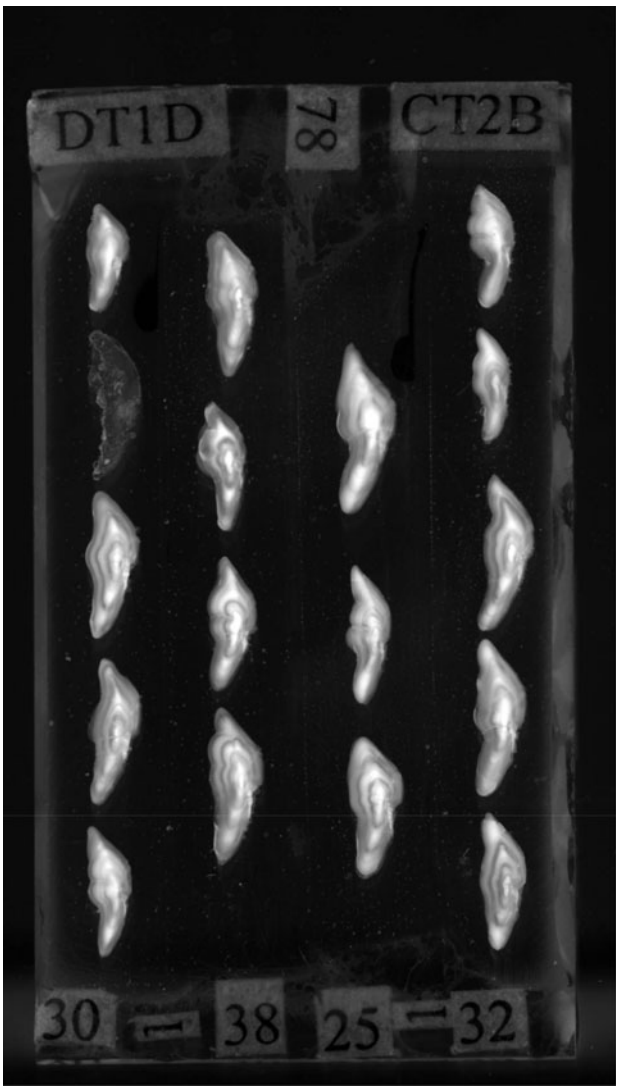

Fig. S3. Preparations of otolith sections, randomized to reduce session effects, mounted in resin, polished, and cleaned prior to analysis by laser ablation inductively coupled mass spectrometry (LA-ICPMS). Data from otolith 31 (second from top in left-hand column) was excluded because otolith material was predominantly vaterite

Finnigan Element 2) at the Department of Earth Science, University of Bergen, Norway. Discrete points were sampled with a 213 nm UV laser ablation unit (New Wave UP213), which delivered the vaporised otolith material to the ICPMS. Three discrete spots representing the core area of the otolith (spawning location), and 3 discrete spots representing the otolith edge or surface (harvest location) (Fig. S4) were sampled. The laser spot diameter was 30 µm. For each spot the initial wash time was 30 s and the dwell time 84 s (divided equally across 15 isotopes: Li7, Na23, Mg24, Mg25, Ca43, Ti47, Mn55, Ni62, Cu63, Cu65, Rb85, Sr86, Sr88, Ba137, and Pb208). Samples were analyzed together with 2 multi-element reference materials (SRMs), NIST glass 612, and BCR carbonate.

Quanitative results were obtained by offline signal processing using GLITTER software (ARC National Key Centre for Geochemical Evolution and Metallogeny of Continents, Macquarie University; Van Achterbergh et al. 2001), based on the analytical standards, and all results are reported in µg g^{-1}.

A quality-control procedure was developed to screen for laser spots affected by heterogeneous and irregular features in the otolith that can cause aberrant results. All data points below the limit of detection were set to the limit of detection. The 3 data points taken close together at either the core or the edge were examined together, and any that were clearly outliers were removed. Vaterite areas of the otoliths were immediately identified by the high concentrations of Mg and low concentrations of Sr, and these spots were removed entirely from the analysis, even though the concentrations of the other elements appeared to be unaffected. The performance of the analysis was also monitored by comparing measured and certified concentrations in reference materials. Several elements (Li7, Ti47, and Ni62) were excluded from the analysis after the quality-control examination showed that the measurements were not reliable throughout the data set.

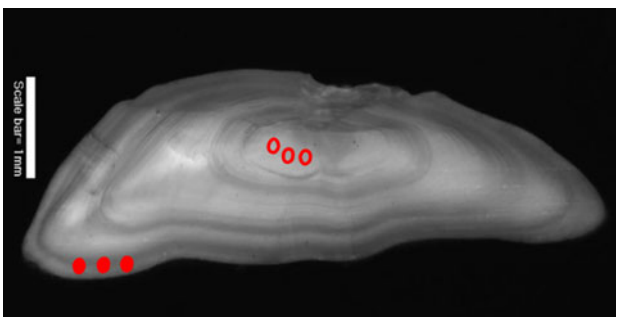

Fig. S4. Cod otolith sectioned through the core region and prepared for LA-ICPMS analysis. ○: laser ablation sampling of otolith core composition representing spawning location. ●: laser ablation sampling of otolith edge/surface composition representing harvest location

Otolith concentration data were examined for normality within each sample group (season, area), and also for dependence on fish length and age. Where needed, the concentration values were standardized by using the residuals of the element concentration/fish length relationship. This was the case for Mg, Mn, Sr, and Ba.

The otolith composition (concentrations of Na, Mg, Mn, Cu, Rb, Sr, Ba, and Pb) was compared by ANOVA between the fish sampled from different areas and seasons. Significant differences were evaluated post hoc by Tukey's test. Discriminant analysis was used to build a classification model and to calculate the probability of assignment of individuals to each group. Assignments and classification success were cross-validated by the 'leave-one-out' method, where each fish was classified by the model determined from all fish excluding that one. The most important elements in the discriminant model were Rb, Mn, Sr, Ba, and classification success ranged from 71% for cod from the Baltic to 38% for cod from the Celtic Sea.

LITERATURE CITED

Applied Biosystems (2000). GeneScan analysis, version 3.1.2. Applied Biosystems, Foster City, CA

Applied Biosystems (2002). GeneMapper, version 3.0. Applied Biosystems, Foster City, CA

Begg G, Brown R (2000) Stock identification of haddock *Melanogrammus aeglefinus* on Georges Bank based on otolith shape analysis. Trans Am Fish Soc 129:935–945

Brooker AL, Cook D, Bentzen P, Wright JM, Doyle RW (1994) Organization of microsatellites differs between mammals and cold-water teleost fishes. Can J Fish Aquat Sci 51: 1959–1966

Campana SE, Casselman JM (1993) Stock discrimination using otolith shape analysis. Can J Fish Aquat Sci 50: 1062–1083

Cardinale M, Doering-Arjes P, Kastowsky M, Mosegaard H (2004) Effects of sex, stock and environment on the shape of known-age Atlantic cod (*Gadus morhua*) otoliths. Can J Fish Aquat Sci 61:158–167

Galley EA, Wright PJ, Gibb FM (2006) Combined methods of otolith shape analysis improve identification of spawning areas of Atlantic cod. ICES J Mar Sci 63:1710–1717

Hemmingsen W, MacKenzie K (2001) The parasite fauna of the Atlantic cod, *Gadus morhua* L. Adv Mar Biol 40:1–80

Miller KM, Le KD, Beacham TD (2000) Development of tri- and tetranucleotide repeat microsatellite loci in Atlantic cod (*Gadus morhua*). Mol Ecol 9:238–239

O'Reilly PT, Canino MF, Bailey KM, Bentzen P (2000) Isolation of twenty low stutter di- and tetranucleotide microsatellites for population analyses of walleye pollock and other gadoids. J Fish Biol 56:1074–1086

Ponton D (2006) Is geometric morphometrics efficient for comparing otolith shape of different fish species? J Morphol 267:750–757

Smith PJ, Robertson SG, Horn PL, Bulla B, Anderson OF, Stantona BR, Okec CS (2002) Multiple techniques for determining stock relationships between orange roughy, *Hoplostethus atlanticus*, fisheries in the eastern Tasman Sea. Fish Res 58:119–140

SPSS Inc (1999) Neural Connection, version 2.0. Chicago
Strauss RE, Bookstein FL (1982) The truss-body form reconstructions in morphometrics. Syst Zool 31:113–135
Tabachnick B, Fidell LS (1996) Using multivariate statistics. Addison Wesley, Pearson Education, Upper Saddle River, NJ
Van Achterbergh E, Ryan CG, Griffin WL (2001) GLITTER Version 4 user's manual. On-line interactive data reduction for the LA-ICPMS microprobe. In: Paul Sylvester (ed): Laser-ablation-ICPMS in the earth sciences — principles and applications. Mineralogical Association of Canada. Short Course 29:239–243
Van Heel M, Harauz G, Orlova EV, Schmidt R, Schatz M (1996) A new generation of the IMAGIC image processing system. J Struct Biol 116:17–24
Walsh PS, Metzger DA, Higuchi R (1991) Chelex 100 as a medium for simple extraction of DNA for PCR-based typing from forensic material. Biotechniques 10:506–513